

Interrelation between Light Emitting and Structural Properties of Si Nanoclusters Embedded in SiO₂ and Al₂O₃ Hosts

L. Khomenkova, O. Kolomys, V. Strelchuk, A. Kuchuk, V. Kladko, M. Baran, J. Jedrzejewski, I. Balberg, P. Marie, F. Gourbilleau, N. Korsunskaya

Published online by Cambridge University Press 19 Nov 2013:

MRS Online Proceedings Library, Volume 1617, January 2013, imrc2013-s7e-0013
doi: 10.1557/opl.2013.1167

Interrelation between Light Emitting and Structural Properties of Si Nanoclusters Embedded in SiO₂ and Al₂O₃ Hosts

L. Khomenkova¹, O. Kolomys¹, V. Strelchuk¹, A. Kuchuk¹, V. Kladko¹, M. Baran¹,
J. Jedrzejewski³, I. Balberg³, P. Marie², F. Gourbilleau², N. Korsunskaya¹

¹V. Lashkaryov Institute of Semiconductor Physics, 45 Pr. Nauky, Kyiv 03028, Ukraine

²CIMAP/ENSICAEN, 6 Blvd. Maréchal Juin, 14050 Caen cedex 4, France

³Racah Institute of Physics, Hebrew University, 91904 Jerusalem, Israel

ABSTRACT

The present work deals with the comparative investigation of Si-ncs embedded in SiO₂ and Al₂O₃ dielectrics grown by RF magnetron sputtering on fused quartz substrate. The effect of post-deposition processing on the evolution of microstructure of the films and their optic and luminescent properties was investigated. It was observed that photoluminescence (PL) spectra of Si_x(SiO₂)_{1-x} films showed one PL band, which peak position shifts from 860 nm to 700 nm when the x decreases from 0.7 to 0.3. It is due to exciton recombination in Si-ncs. For Si_x(Al₂O₃)_{1-x} films, several PL bands peaked at about 570-600 nm and 700-750 nm and near-infrared tail or band peaked at about 800 nm were found. Two first PL bands were ascribed to different oxygen-deficient defects of oxide host, whereas near-infrared PL component is due to exciton recombination in Si-ncs. The comparison of both types of the samples showed that the main radiative recombination channel in Si_x(SiO₂)_{1-x} films is exciton recombination in Si-ncs, while in Si_x(Al₂O₃)_{1-x} films the recombination via defects prevails due to higher amount of interface defects in the Si_x(Al₂O₃)_{1-x} caused by stresses.

INTRODUCTION

The realization of low-cost integrated optoelectronic devices fully based on well-developed Si-based CMOS technology (i.e. all-in-one Si chip) is important task. In this regard, silicon nanocrystallites (Si-ncs) attract considerable interest due to significant transformation of their optical and electrical properties caused by quantum-confinement effect [1,2]. Being embedded in dielectric hosts, Si-ncs offer potential applications in optoelectronic devices that were demonstrated during last decades for Si-ncs-SiO₂ systems [3,4,5,6].

However, the downscaling of microelectronic devices requires the elaboration of novel materials to overcome bottleneck of silicon oxide as a gate material. In this regard, other dielectrics such as ZrO₂, HfO₂ and Al₂O₃ are considered as promising gate dielectrics [7]. It was also demonstrated that Si-ncs embedded in such high-k host offer a wider application for non-volatile memories due to the higher performance of the corresponding devices [8,9].

Among different dielectrics, Al₂O₃ is not well addressed as photonic material. At that, it has relatively higher refractive index (1.73 at 1.95 eV) in comparison with that of SiO₂ (1.46 at 1.95 eV) at similar band gap energies offering better light confinement, making compact device structures possible. It was shown an application of alumina-based waveguides fabricated by sol-gel techniques for optical communication. Few reports on Si-ncs-Al₂O₃ materials fabricated by ion implantation or electron beam evaporation are also available [10,11,12]. At the same time, magnetron sputtering was not often considered for fabrication of Al₂O₃ materials with embedded

Si-ncs [13,14,15] in spite of the relative simplicity of this approach and its wide application for the fabrication of Si-ncs-SiO₂ films [5,9].

The present paper demonstrates the application of magnetron sputtering for the fabrication of Si-rich-Al₂O₃ and Si-rich-SiO₂ films with different Si content. The effect of post-deposition processing on the evolution of microstructure of the films and their optic and luminescent properties was observed.

EXPERIMENT

The Si_x(Al₂O₃)_{1-x} and Si_x(SiO₂)_{1-x} films with 0.15 ≤ x ≤ 0.7 were deposited by radio frequency magnetron co-sputtering of two spaced-apart targets (pure Si and pure oxide (Al₂O₃ or SiO₂)) in pure argon plasma on a long silicon oxide substrate at room temperature. More details can be found elsewhere [15,16]. The as-deposited original films were annealed at 1150°C during 30 min in nitrogen flow to form the Si-ncs in oxide hosts.

To investigate the microstructure and luminescent properties of the films, a Horiba Jobin-Yvon T-64000 Raman spectrometer equipped with confocal microscope and automated piezo-driven XYZ stage was used. The Raman scattering and photoluminescence spectra were detected in 100-900-cm⁻¹ and in 500-900-nm spectral ranges, respectively. A 488.0-nm line of Ar-Kr ion laser was used as the excitation source. The laser power on the sample surface was always kept below 5 mW to obtain the best signal-to-noise ratio, preventing a laser heating of the investigated sample. The spectral resolution of the spectrometer was less than 0.15 cm⁻¹. To study the chemical composition of the films (x), their refractive index and thickness, the spectroscopic ellipsometry measurement was performed by means of a Jobin-Yvon ellipsometer (UVISEL), where the incident light was scanned in the range 1.5-4.5 eV under an incident angle of 66.3°. [7,13]. The electron paramagnetic resonance (EPR) spectra were measured by means Varian-12 spectrometer to obtain the information about the defect structure of the samples. The investigations were performed at 300 K.

RESULTS

Raman scattering study of as-deposited Si_x(Al₂O₃)_{1-x} and Si_x(SiO₂)_{1-x} films with the x ≥ 0.35 revealed the presence of amorphous silicon (a-Si) phase (Fig.1a). Besides, the shift of peak position of the transverse optic (TO) band to ω_{TO-a-Si}=460cm⁻¹ was observed for Si_x(Al₂O₃)_{1-x} films contrary to that detected for Si_x(SiO₂)_{1-x} counterparts (ω_{TO-a-Si}=480cm⁻¹). This latter corresponds to the TO phonon peak position of relaxed amorphous silicon. The low-frequency shift observed for Si_x(Al₂O₃)_{1-x} samples can be ascribed to tensile stresses between the film and fused quartz substrate due to mismatching between lattice parameters of fused quartz and the film. It is obvious that this effect is negligible for the Si_x(SiO₂)_{1-x} films.

Annealing treatment at T_A=1150°C results in the increase of TO phonon band intensity and its narrowing that is the evidence of Si-ncs formation in both types of the samples (Fig.1b). When the x decreases, the shift of the ω_{TO-nc-Si} to the lower wavenumbers occurs for Si_x(SiO₂)_{1-x} (Fig.1b, inset) that can be ascribed to the decrease of Si-ncs sizes.

In all Si_x(Al₂O₃)_{1-x} samples, the ω_{TO-nc-Si} is shifted to lower wavenumbers (517.3-518.7 cm⁻¹) in comparison with the peak position of TO phonon band of bulk Si (ω_{TO-bulk-Si}=521 cm⁻¹). But contrary to Si_x(SiO₂)_{1-x} films, for Si_x(Al₂O₃)_{1-x} samples with x=0.55-0.7 only slight shift of the ω_{TO} towards the higher wavenumbers is detected with x decrease (Fig.1b, inset). It is worth to note that along with Si crystalline phase, the amorphous Si phase was also detected in annealed

samples. However, for the samples with the same x values its contribution is lower for the $\text{Si}_x(\text{Al}_2\text{O}_3)_{1-x}$ samples than for $\text{Si}_x(\text{SiO}_2)_{1-x}$ counterparts.

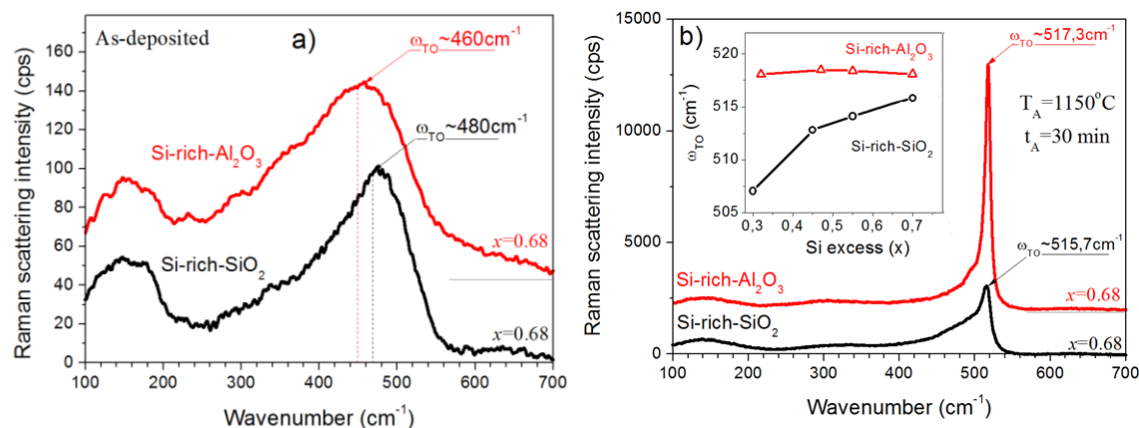


Fig.1. Raman scattering spectra as-deposited (a) and annealed (b) $\text{Si}_x(\text{SiO}_2)_{1-x}$ and $\text{Si}_x(\text{Al}_2\text{O}_3)_{1-x}$ films with $x=0.68$. The inset in Fig.1b shows variation of TO phonon peak position versus x for both types of samples.

The presence of amorphous Si phase in as-deposited samples was also revealed by EPR measurements. They showed for both types' samples with $x \geq 0.35$ a significant contribution of the signal with $g=2.0055$. This latter corresponds to the silicon dangling bonds. Its intensity reflects the total number of these centers and decreases with x decrease. Annealing treatment results in the transformation of EPR spectra of both types of samples.

For $\text{Si}_x(\text{SiO}_2)_{1-x}$ films with $x > 0.35$, an asymmetric signal with $g=2.0057$, which intensity increase with x , was found. Besides, for the layers with $x > 0.55$ slight dependence of EPR spectra on the orientation of magnetic field was detected. Since annealed $\text{Si}_x(\text{SiO}_2)_{1-x}$ films contain both Si-ncs and amorphous Si phase, this signal is obviously a superposition of two signals, i.e. P_b -like centers that are the feature of Si/SiO₂ interface formation, and Si dangling bonds. Slight anisotropy of EPR signal and the increase of the g -factor value are additional arguments for the formation of P_b -like centers. Annealed $\text{Si}_x(\text{Al}_2\text{O}_3)_{1-x}$ samples showed also the signal with $g_1=2.0057$ attributed to the superposition of Si dangling bonds and P_b -like centers that can be the feature of both Si/SiO₂ and Si/Al₂O₃ interfaces [16].

Any emission was not observed for as-deposited $\text{Si}_x(\text{SiO}_2)_{1-x}$ films, whereas weak PL emission in orange spectral range was detected from $\text{Si}_x(\text{Al}_2\text{O}_3)_{1-x}$ films with $x < 0.5$. Similar PL emission was also observed in pure Al₂O₃ film and can be assigned to F_2^{2+} centers in Al₂O₃ [17]. Annealing of $\text{Si}_x(\text{SiO}_2)_{1-x}$ films results in the appearance of one broad PL band in red-near-infrared spectral range (Fig.2a). Its peak position shifts from 1.4 eV to 1.8 eV when the x decreases from 0.45 to 0.3 and does not change for $x > 0.5$ (Fig.2a, inset). Annealed $\text{Si}_x(\text{Al}_2\text{O}_3)_{1-x}$ films demonstrate the PL spectrum in wider spectral range (Fig.2b). These spectra contain two broad PL bands with maxima at 2.06-2.18 eV and 1.65-1.77 eV accompanied by near-infrared tail or weak band (1.55-1.60 eV). These bands can be well-separated (for $x=0.45-0.5$) or strongly overlapped. The first band consists of two components with maxima positions at ~ 2.06 eV and ~ 2.18 eV. The latter one is clearly seen in the sample with $x=0.3$ and is similar to PL emission from F_2^{2+} centers in Al₂O₃ [18]. Furthermore, this PL band presents in other spectra also,

testifying that the Si-ncs are incorporated into Al_2O_3 matrix. At the same time, both components are strongly overlapped in the samples with $x > 0.3$ (Fig.2).

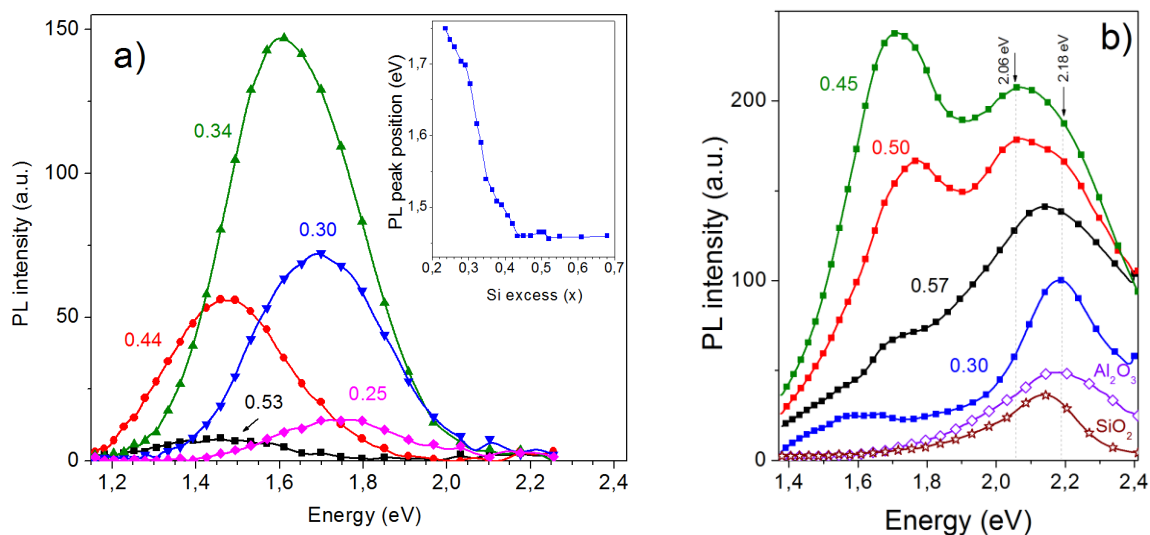


Figure 2. Room-temperature PL spectra of $\text{Si}_x(\text{SiO}_2)_{1-x}$ (a) and $\text{Si}_x(\text{Al}_2\text{O}_3)_{1-x}$ (b) films. The values of the x are mentioned in the figures. Excitation wavelength is 488 nm.

DISCUSSION

The investigation of structural properties of as-deposited $\text{Si}_x(\text{SiO}_2)_{1-x}$ and $\text{Si}_x(\text{Al}_2\text{O}_3)_{1-x}$ films showed that one of their specific features is the presence of amorphous Si phase for the samples with $x > 0.35$. Besides, the $\text{Si}_x(\text{Al}_2\text{O}_3)_{1-x}$ films are stressed contrary to $\text{Si}_x(\text{SiO}_2)_{1-x}$ ones. These stresses are tensile and caused by the mismatching in the lattice constants of fused quartz substrate and the film. Raman scattering data shows also that after annealing treatment the Si-ncs in $\text{Si}_x(\text{Al}_2\text{O}_3)_{1-x}$ samples are stressed. In fact, the peak position of TO phonon band of the Si-ncs for the samples with $x > 0.5$ is shifted to the lower frequency side ($\omega_{\text{TO-nc-Si}} = 517\text{-}518\text{ cm}^{-1}$) in comparison with that for bulk Si ($\omega_{\text{TO-bulk-Si}} = 521\text{ cm}^{-1}$). At the same time, the mean size of Si-ncs, estimated from XRD data, is about 14 nm [15]. It is obvious that the contribution of phonon quantum confinement effect is negligible in this case. This means that the Si-ncs in the $\text{Si}_x(\text{Al}_2\text{O}_3)_{1-x}$ samples are under tensile stress contrary to the Si-ncs in the $\text{Si}_x(\text{SiO}_2)_{1-x}$ films. This is in agreement with Raman scattering data obtained for as-deposited samples.

As it was mentioned the peak position of Raman band of the Si-ncs for $\text{Si}_x(\text{Al}_2\text{O}_3)_{1-x}$ in the samples with $x > 0.55$ shifts slightly to high frequency side with the x decrease that cannot be caused by the change of crystallite sizes because the decrease of Si content should result in the decrease of Si crystallites and lead to opposite shift of Raman line. The observed shift is obviously caused by the decrease of amorphous Si phase content that is in agreement with the decrease of intensity of TA phonon of amorphous Si ($\omega_{\text{TA-a-Si}} = 150\text{ cm}^{-1}$). Thus, the sizes of Si-ncs in $\text{Si}_x(\text{Al}_2\text{O}_3)_{1-x}$ films cannot be estimated from Raman data.

Another situation occurs in the $\text{Si}_x(\text{SiO}_2)_{1-x}$ films. With the x decrease the shift of the $\omega_{\text{TO-nc-Si}}$ to the lower wavenumbers occurs (Fig.1b, inset). Besides, the increase of full-width at half maximum of this phonon band is observed (not shown). The sizes of Si-ncs embedded in SiO_2 host can be estimated from the fitting of Raman scattering spectra. Based on such analysis the

increase of Si-ncs mean size from ~2.7 nm to 6.0 nm was found for $\text{Si}_x(\text{SiO}_2)_{1-x}$ samples when the x increases from 0.3 to 0.5, whereas for $x > 0.5$, Si-ncs size does not change practically. These results are in a good agreement with XRD data obtained earlier.

Present results showed also that mean size of Si-ncs in Al_2O_3 exceeds that for Si-ncs in SiO_2 for the films with same x values. One of the reasons of this phenomenon can be faster diffusion of Si in alumina than that in silica in the case when Si-ncs formation is determined by Si diffusion towards Si-nuclei and their Ostwald ripening. Another reason can be lower temperature required for phase separation in $\text{Si}_x(\text{Al}_2\text{O}_3)_{1-x}$ than that for $\text{Si}_x(\text{SiO}_2)_{1-x}$. In spite of the difference in Si-ncs sizes these films have one trait in common. For the samples with $x > 0.5$ the mean Si-ncs sizes do not change with x . This can be connected with presence of amorphous Si inclusions in as-deposited films. In this case their crystallization can contribute to appearance of Si-nc besides the process of phase separation. For $x > 0.5$ this contribution can be crucial. If these inclusions are big enough (that can be expected for high Si excess) the crystallite sizes will be determined by the temperature and duration of annealing only as for amorphous Si films crystallization. Indeed, rapid thermal annealing of $\text{Si}_x(\text{Al}_2\text{O}_3)_{1-x}$ samples results in the formation of smaller Si-ncs, but their mean size was found to be independent on x for $x > 0.5$ [13,14].

Raman scattering spectra of annealed films showed also the higher relative contribution of amorphous Si phase in $\text{Si}_x(\text{SiO}_2)_{1-x}$ than in $\text{Si}_x(\text{Al}_2\text{O}_3)_{1-x}$. This can be due to lower temperature for the crystallization of amorphous Si clusters in Al_2O_3 host compared with that in SiO_2 and is in the agreement with the data of Ref. [10].

Significant difference in PL properties of $\text{Si}_x(\text{SiO}_2)_{1-x}$ and $\text{Si}_x(\text{Al}_2\text{O}_3)_{1-x}$ films was observed. For $\text{Si}_x(\text{SiO}_2)_{1-x}$ films, evolution of PL peak position versus x correlates with the variation of Si-ncs mean size. This allows ascribing it to exciton recombination in Si-ncs. Thus, in these films exciton recombination in Si-ncs is dominant radiative channel.

At the same time several radiative channels are observed in $\text{Si}_x(\text{Al}_2\text{O}_3)_{1-x}$ films. The investigation of temperature behavior of PL spectra showed that the peak positions and the intensities of PL components peaked at 2.06-2.15 eV and 1.65-1.77 eV do not change with cooling [13]. This allowed ascribing them to radiative recombination of carriers through the defects of matrix and/or Si-ncs/host interface states. They are F-like centers in Al_2O_3 emitted at ~2.06 eV [19] and ~2.18 eV [18]. It is worth to note that PL components at ~1.65-1.77 eV and ~2.06 eV were observed only when Si-ncs are present in the film. This can be explained by their location near Si-ncs or at Si-ncs/host interface.

The contribution of near-infrared tail or band peaked at about 1.55 eV increases with cooling [13,14] that is typical feature of Si-ncs exciton PL band. However, its PL intensity is much lower than the emission of oxide-related defects contrary to that observed in $\text{Si}_x(\text{SiO}_2)_{1-x}$ films. This can be due to high number of non-radiative defects at Si-ncs/ Al_2O_3 interface which, in particular, can appear due to mechanical stress in $\text{Si}_x(\text{Al}_2\text{O}_3)_{1-x}$ films.

CONCLUSIONS

RF magnetron sputtering approach was used for deposition of $\text{Si}_x(\text{SiO}_2)_{1-x}$ and $\text{Si}_x(\text{Al}_2\text{O}_3)_{1-x}$. The investigation of structural and light emitting properties of these films allowed getting the information about the Si-ncs formation and the nature of the emitting centers in the films with different Si content. Comparative analysis of PL spectra of both types' samples showed that the main contribution to PL spectra of $\text{Si}_x(\text{SiO}_2)_{1-x}$ films is given by exciton recombination in the Si-ncs whereas PL emission of $\text{Si}_x(\text{Al}_2\text{O}_3)_{1-x}$ films is caused mainly by carrier recombination either via defects in matrix or via electron states at the Si-ncs/matrix interface.

ACKNOWLEDGMENTS

This work was supported by the National Academy of Sciences of Ukraine and Ministry of Art and Science of Israel.

REFERENCES

1. Canham LT: Appl Phys Lett 1990, 57:1046-1048.
2. Lehman V, Gosele U: Appl Phys Lett 1991, 58:856-858.
3. X.Y.Chen, Y.F.Lu, Tang LJ, Wu YH, Cho BJ, Xu XJ, Dong JR, Song WD: J Appl Phys 2005, 97:014913.
4. Khomenkova L, Korsunska N, Yukhimchuk V, Jumaev B, Torchinska T, Vivas Hernandez A, Many A, Goldstein Y, Savir E, Jedrzejewski J: J Lumin 2003, 102/103:705.
5. Baran N, Bulakh B, Venger Ye, Korsunska N, Khomenkova L, Stara T, Goldstein Y, Savir E, Jedrzejewski J: Thin Solid Films 2009, 517:5468.
6. Qin GG, Liu XS, Ma SY, Lin J, Yao GQ, Lin XY, Lin KX: Phys Rev B 1997, 55:12876.
7. Khomenkova L, Portier X, Cardin J, Gourbilleau F: Nanotechnology 2010, 21: 285707.
8. Steimle RF, Muralidhar R, Rao R, Sadd M, Swift CT, Yater J, Hradsky B, Straub S, Gasquet H, Vishnubhotla L, Prinz EJ, Merchant T, Acred B, Chang K, White Jr BE: 2007, 47:585.
9. Baron T, Fernandes A, Damlencourt JF, De Salvo B, Martin F, Mazen F, Haukka S: Appl Phys Lett 2003, 82: 4151.
10. Mikhaylov AN, Belov AI, Kostyuk AB, Zhavoronkov IYu, Korolev DS, Nezhdanov AV, Ershov AV, Guseinov DV, Gracheva TA, Malygin ND, Demidov ES, Tetelbaum DI: Physics of the Solid State (St.Petersburg, Russia) 2012, 54:368.
11. Yerci S, Serincan U, Dogan I, Tokay S, Genisel M, Aydinli A, Turan R: J Appl Phys 2006, 100:074301.
12. Núñez-Sánchez S, Serna R, García López J, Petford-Long AK, Tanase M, Kabius B: J Appl Phys 2009, 105:013118.
13. N.Korsunska, T.Stara, V.Strelchuk, O.Kolomys, V. Kladko, A.Kuchuk, B.Romanyuk, O.Oberemok, J.Jedrzejewski, P. Marie, L.Khomenkova, I.Balberg, Nanoscale Research Letters, 2013, 8: 273.
14. N. Korsunska, T. Stara, V. Strelchuk, O. Kolomys, V. Kladko, A. Kuchuk, L. Khomenkova, J. Jedrzejewski, I. Balberg, Physica E, 2013, 51: 115.
15. L.Bi, J.Y. Feng: J Lumin 2006, 121:95.
16. B.J. Jones, R.C. Barklie, J.Pys.D.:Appl.Phys. 2005, 38:1178.
17. S. Yin, E. Xie, C. Zhang, Z. Wang, L. Zhou, I.Z. Ma, C.F. Yao, H. Zang, C.B. Liu, Y.B. Sheng, J. Gou, Nucl Instr Methods B 2008, 12-13:2998.
18. Y.Song, C.H.Zhang, Z.G. Wang, Y.M. Sun, J.L. Duan, Z.M. Zhao, Nucl. Instr.Meth.Phys.Res.B 2006, 245:210.
19. Dogan I, Yildiz I, Turan R: Physica E 2009, 41:976.